Revista Brasileira de Ciência do Solo
ISSN: 0100-0683
revista@sbcs.org.br
Sociedade Brasileira de Ciência do Solo
Brasil

da Silva, Márcio Luiz; Batezelli, Alessandro; Bernardes Ladeira, Francisco Sérgio
Micromorphology of Paleosols of the Marília Formation and their Significance in the Paleoenvironmental Evolution of the Bauru Basin, Upper Cretaceous, Southeastern Brazil
Revista Brasileira de Ciência do Solo, vol. 41, 2017, pp. 1-20
Sociedade Brasileira de Ciência do Solo
Viçosa, Brasil

Revista Brasileira de Ciência do Solo

Division – Soil in Space and Time | Commission – Soil Genesis and Morphology

Micromorphology of Paleosols of the Marília Formation and their Significance in the Paleoenvironmental Evolution of the Bauru Basin, Upper Cretaceous, Southeastern Brazil

Márcio Luiz da Silva[(1)*], Alessandro Batezelli[(2)] and Francisco Sérgio Bernardes Ladeira[(3)]

[(1)] Instituto Federal de Educação, Ciência e Tecnologia do Sul de Minas, *Campus* Inconfidentes, Inconfidentes, Minas Gerias, Brasil.
[(2)] Universidade Estadual de Campinas, Departamento de Geologia e Recursos Naturais, Instituto de Geociências, Campinas, São Paulo, Brasil.
[(3)] Universidade Estadual de Campinas, Departamento de Geografia, Instituto de Geociências, Campinas, São Paulo, Brasil.

ABSTRACT: Deduction of associated paleoenvironments and paleoclimate, definition of the chronosequence of paleosols, and paleogeographic reconstruction have become possible through the application of micromorphology in paleopedology. Micromorphology has also been useful in recognition of weathering processes and definition of minerals formed in succession. In this respect, the objective of this study was to identify the development of pedogenic processes and discuss their significance in the paleoclimate evolution of the Marília Formation (Maastrichtian) of Bauru Basin. Three sections of the Marília Formation (A1, A2, and A3) were described, comprising nine profiles. Micromorphologic al analysis was carried out according to the specialized literature. In the Marília Formation, the paleosols developed in sandstones have argillic (Btkm, Bt) and carbonate (Bk) horizons with different degrees of cementation, forming mainly calcretes. The evolution of pedogenic processes, in light of micromorphological analysis, evidenced three moments or stages for the genesis of paleosols with Bkm, Btk, and Bt horizons, respectively. In the Maastrichtian in the Bauru Basin, the paleosols with Bkm are older and more arid environments, and those with Bt were formed in wetter weather, but not enough to lead to the genesis of enaulic-related distributions, typical of current Oxisols.

Keywords: Calcrete, c/f-related distribution, b-fabric, pedofeatures, paleoclimate.

*** Corresponding author:**
E-mail: marcgeo10@yahoo.com.br

Received: July 13, 2016
Approved: July 27, 2016

How to cite: Silva ML, Batezelli A, Ladeira FSB. Micromorphology of Paleosols of the Marília Formation and their Significance in the Paleoenvironmental Evolution of the Bauru Basin, Upper Cretaceous, Southeastern Brazil. Rev Bras Cienc Solo. 2017;41:e0160287.

INTRODUCTION

Micromorphology or micropedology can be defined as the branch of soil science that deals with the description, interpretation and, to some extent, the measure of soil constituents, features, and fabrics at the microscopic level (Bullock et al., 1985). Among its main objectives, micromorphological analysis allows us to formulate hypotheses or statements about the genetic and evolutionary dynamics of soil in an attempt to clarify controversy regarding its origin, evolution, and behavior (Castro et al., 2003). The identification of different constituents of the soil in different fractions, as well as definition of possible interrelationships between them, is another key objective of micromorphology (Castro et al., 2003).

One of the applications of micromorphology is to identify the pedogenetic process and display transfers and concentrations of elements (eluviation, illuviation, nodulation, or concretion) and to follow the development of distinctive features (porosity and pedoturbation, among others). It can also be applied in recognition of the weathering process involved and the mineral succession formed (Delvigne, 1998). The transformation of saprolite to soil, called pedoplasmation, is another topic that can be studied by micromorphology, as it concerns in the first place the transformation of fabrics, initially without mineralogical or chemical changes (Stoops, 2008).

In paleopedology, micromorphology may be useful in deduction of paleoenvironments and associated paleoclimates, the chronosequence of paleosols, and paleogeographic reconstitution (Porta et al., 1999).

Paleosols are defined as soils that were formed on an ancient landscape (Wright, 1986). They may be buried soils and/or soils incorporated into the sedimentary sequences, exhumed soils, or soils developed on ancient relief surfaces (relict soils) (Andreis, 1981; Catt, 1990). Exposed on the surface and influenced by later environmental changes (Retallack, 2001), paleosols reveal ancient environments and contain records regarding the climate, vegetation, landforms, intensity of pedogenesis, and sedimentation rates in effect during their training (Kraus, 1992; Wright, 1992).

Paleosols have been used both in analysis and paleoenvironmental reconstructions (Andreis, 1981; Catt, 1990; Retallack, 2001; Sheldon and Tabor, 2009; Nascimento et al., 2017) by forming themselves into open systems capable of recording environmental conditions during their training, as in stratigraphic correlation (Brown and Kraus, 1988; Wright, 1992; Marriott and Wright, 1993; Kraus 1997; McCarthy and Plint, 2003), indicating a stable surface and representing moments of pause in erosion and deposition.

However, paleosols are often difficult to identify since various physical and chemical properties change as a result of weathering processes and infiltration of solutions. However, micromorphological features are well preserved and allow determination of the type of soil, the environment, and the associated paleoclimate (Stoops, 2008). Thus, micromorphology has become an important tool in studies on global climate change.

In the Marília Formation, the paleosols developed on sandstones have argillic (Btk, Bt) and calcic (Bk) horizons with different degrees of cementation, forming mainly calcretes.

Groundmass and coating features, hypocoatings, quasicoatings, and infillings reveal the pedological nature of calcretes as a result of *in situ* weathering, allowing determination of chronology, intensity of processes, and the climatic conditions of their occurrence.

Studies of micromorphological features reveal pedogenic processes and assist in the interpretation of paleoclimatic environments.

Thus, the objective of this study was to identify, through micromorphology, the development of pedogenic processes in paleosols of the Marília Formation and discuss their significance in paleoclimatic evolution of the Maastrichtian of the Bauru Basin, southeastern Brazil.

MATERIALS AND METHODS

Characterization of the Bauru Basin and study area

The Bauru Basin, located in southeastern Brazil, covers an area of approximately 330,000 km², including the middle west of São Paulo, northeastern Mato Grosso do Sul, southern Mato Grosso, southern Goiás, and western Minas Gerais (Figure 1). This basin has an elliptical shape, elongated in the N-NE direction, and consists primarily of siliciclastic continental deposits (Batezelli, 2003).

The erosional processes responsible for the current configuration of the Bauru Basin boundaries are relates to tectonic restructuring of the Tertiary. This event is marked on

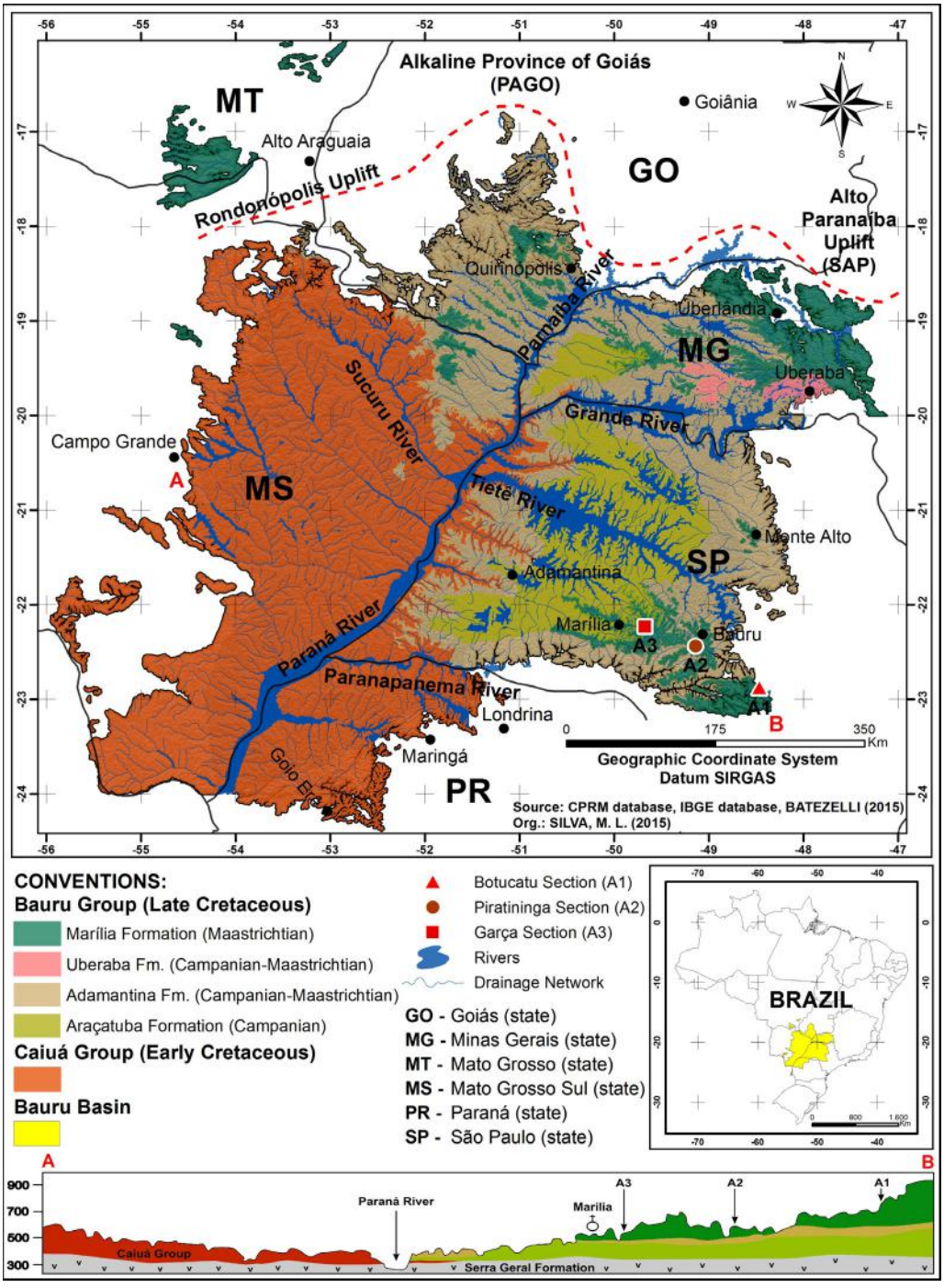

Figure 1. Lithostratigraphic map and geologic section (A-B) of the Bauru Basin. The red square, circle, and triangle are the outcrop positions in the study area.

the eastern border of the Bauru Basin by the Serra do Mar mountain range and Alto Paranaíba Uplift (Batezelli, 2003, 2015).

The Bauru Basin originated in the Late Cretaceous, was developed over the basalt rocks of the Serra Geral Formation, and was generated by flexural subsidence caused by the weight of thick basalt and by Alto Paranaíba Uplift and Alkaline Province of Goiás (Figure 1) (Riccomini, 1995, 1997; Fernandes and Coimbra, 2000; Batezelli 2003; Batezelli et al., 2007; Batezelli, 2010, 2015).

The Bauru Basin developed in the Upper Cretaceous in a period after breakup of the Gondwana continent, and completion occurred in a climate with variations from semi-arid to arid between the Campanian (83.6 to 72.1 Ma B.P) and Maastrichtian (72.1 to 66 Ma B.P.) (Batezelli, 2015).

By analysis of facies, architectural elements, and Paleocurrent, Batezelli et al. (2007) concluded that the deposits of the Bauru Group were formed from unidirectional and gravitational flows of high energy, associated with proximal and intermediate portions of alluvial system dominated by braided rivers (Stanistreet and McCarthy, 1993) or distributive fluvial systems (Hartley et al., 2010) arising from the Alto Paranaíba Uplift and the Alkaline Province of Goiás (Figure 1).

The Bauru Basin is divided into two groups: the Caiuá Group and Bauru Group (Figures 1 and 2). However, there are two different views on the lithostratigraphic position of these two groups. Authors such as Fernandes and Coimbra (1996, 2000) and Fernandes (2004) argue that the two groups are contemporary. Other authors (Fulfaro and Perinotto, 1996; Paula and Silva et al., 2005; Batezelli, 2010, 2015) put the Caiuá Group in the lower portion of the basin, separated from the Bauru Group with a stratigraphic unconformity, signaled by a very evolved paleosol (Geossol Santo Anastásio) highlighted by Fulfaro et al. (1999). Recent studies by Batezelli et al. (2007) and Batezelli (2010, 2015) showed that the two groups are not contemporary (Figure 2), resolving disputes on the stratigraphy of the basin.

The Bauru Group in the state of São Paulo consists of Araçatuba, Adamantina (Vale do Rio do Peixe according to Fernandes and Coimbra, 2000) and Marília (Echaporã Member) formations, from base to top (Batezelli, 2003, 2010, 2015). For Batezelli (2003, 2010, 2015) the Araçatuba Formation was formed in a lacustrine environment (playa-lake) thatserved asthe base level for the river system (generator of the Adamantina and Marília formations). Filling occurred because of the progradational advance of an alluvial system dominated by a braided river that gave rise to the Marília Formation.

Sedimentary evolution of the alluvial system was marked by periods of fluvial sedimentation and aeolian reworking, interspersed with periods of non-deposition (Batezelli, 2010, 2015). During times without deposition, the floodplain would be covered by vegetation and soil could develop. Thus, the Marília Formation consists of a succession of deposits and paleosols that record sedimentation and pedogenesis during the Maastrichtian of the Bauru Basin.

In the Marília Formation, paleosols are constituted by argillic horizons (Btk and Bt) and a calcic horizon (Bk), with different degrees of cementation, constituting calcretes. The irregular distribution and different thicknesses of the profiles are related to the type of the parent material, hydrology, topography, and biology, as well as the exposure time of deposits to weathering agents.

Description of paleosols and sampling

Three sections (A1, A2, and A3) of the Marília Formation (Figure 1) were described, and nine sample profiles collected. Characterization of paleosols was performed according to Retallack (2001) and Santos et al. (2005).

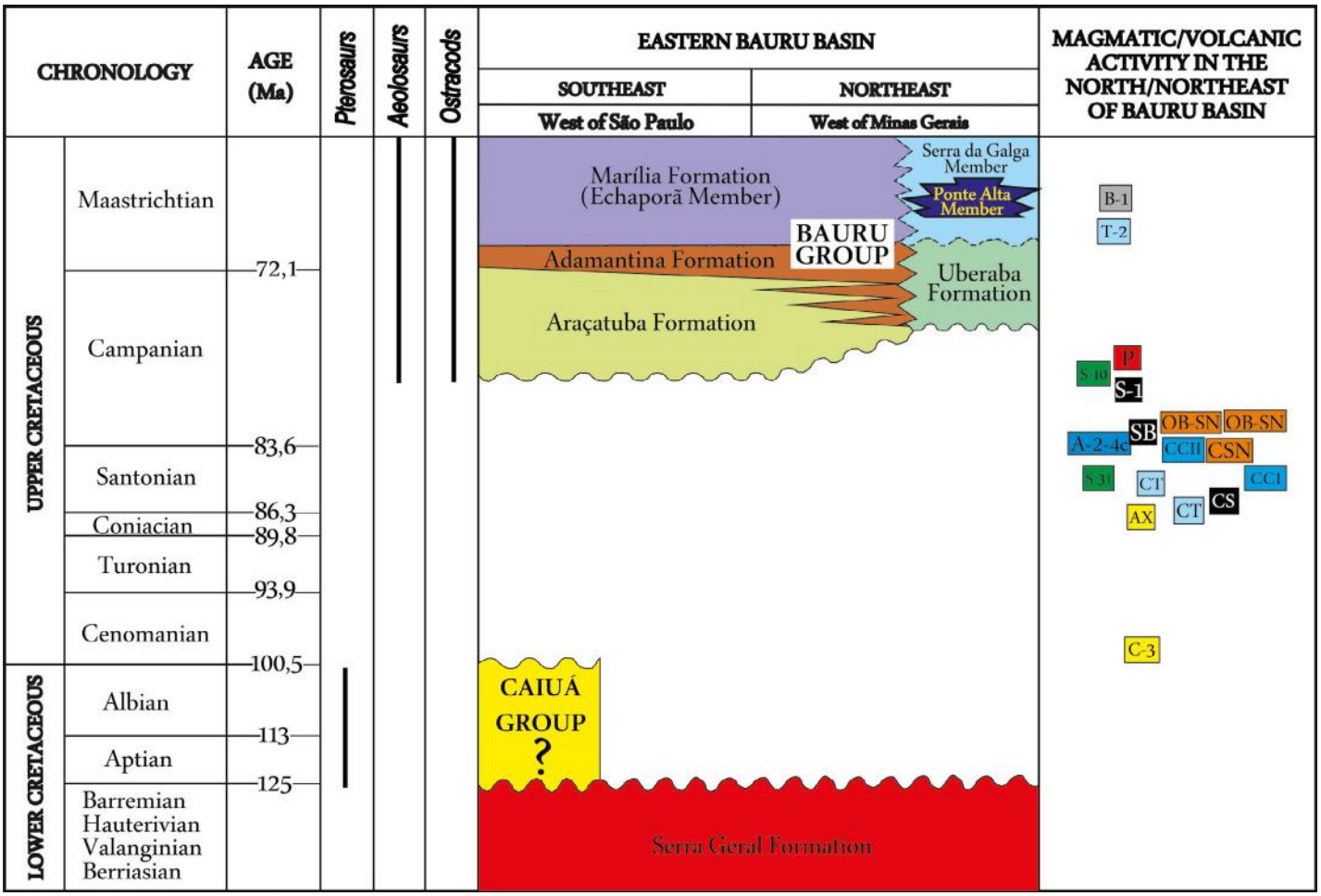

Figure 2. Chronostratigraphic chart of the eastern portion of the Bauru Basin, based on Amaral et al. (1967) (CSN sample); Hasui and Cordani (1968) (samples AX, C-3, S-10, S-31, A-C2-4, OB-SN, SB, S-1, P, T-2, B-1); Sonoki and Garda (1988) (samples CT, CS, CCI); Machado Junior (1992) (sample CCII); Guimarães et al. (2012) and Fragoso et al. (2013) (Pterosaurs); Gobbo-Rodrigues (2001) and Dias-Brito et al. (2001) (Ostracods); Santucci and Bertini (2001) and Martinelli et al. (2011) (Allosaurus). Source: Batezelli (2015).

In characterizing the field, ped structure, horizon, and root marks were identified, the three main attributes in recognition of paleosols (Andreis, 1981; Retallack, 1988; Catt, 1990; Retallack, 2001). To define the horizons, the following types of properties were used: texture, structure, color, thickness, and depth of horizons; types of contacts between paleosol horizons and sediment; presence, type, and size of aggregates (peds); presence and type of films (cutans), presence and type of nodules or cementation; bioturbations; presence or absence of mottling; type, shape, and percentage of root marks; and presence or absence of gleization and friction surfaces (slickensides). Calcic (Bkm) and argillic (Btkm and Bt) horizons have been identified in paleosols of the study area.

The classification of paleosols with Bk horizon in morphological stages of carbonate accumulation followed the method presented by Gile et al. (1966), Machette (1985), Birkeland (1999), and Retallack (2001).

Micromorphological analysis

Description of the oriented thin sections was made according to Bullock et al. (1985) and Stoops (2003) using a binocular magnifying glass to separate domains on the thin section, and a petrographic microscope with magnification of 2.5X to 40X for analysis of the groundmass (s-matrix) and pedofeatures.

The grain size class was determined indirectly by optical microscopy, as proposed by Fitzpatrick (1984) and Bullock et al. (1985).

Scanning electron microscopy analyses were performed on four samples, representative of the different horizons of paleosols.

Interpretations of the groundmass and pedofeatures were based on the studies of Delvigne (1998) and Stoops et al. (2010).

The Visilog 5.4 and Image J 1.48 software was used for processing the images.

RESULTS AND DISCUSSION

Morphological characterization of paleosols

The synthesis of the micromorphological properties of paleosol profiles are summarized in tables 1, 2, and 3.

The identification of pedogenic structures (blocky, prismatic, and laminar) and mark roots, associated with the absence of stratifications, predominance of massive structures, and discontinuity of carbonate cementation on the basis of outcrops, were the main factors used to define the profiles, as being predominantly pedologic. There was a predominance of nodular calcretes, at the expense of powdery (friable), laminar, and hard crust calcretes.

In morphological characterization, paleosols were identified with a Bkm horizon and structure blocks in the Botucatu section (A1), argillic horizons (Btkm and Bt) with prismatic and blocky structure in the Piratininga section (A2), and Btkm and Bkm horizons in the Garça section (A3), with laminar, prismatic, and blocky structures (Figure 3).

Micromorphology

Micromorphology revealed the predominance of porphyric c/f-related distribution in three sections, with some chitonic, enaulic, and gefuric regions.

The paleosols with Bkm horizons showed open porphyric-related distribution with chitonic regions and very few gefuric regions (Table 4, Figure 4a).

Close porphyric-related distribution with chitonic regions predominated in paleosols with Btkm and Bt horizons (Table 4; Figures 4c and 4d).

Table 1. Morphological properties of the paleosols in the Botucatu Section (A1)

Profile and horizon	Depth	EST	Texture	Colors	B	Nodules	RHCl	TRS
	m							
P1Bkm1	0.00-0.42	EB	Sandy (poorly selected)	10YR 8/1, 2.5YR 5/6, 2.5YR 6/6	A	Clasts clay	Reactive	Smooth and clear
P1Bkm2	0.42-0.81	EB	Sandy (poorly selected)	10YR 8/1, 2.5YR 3/6, 2.5YR 5/8	A	Clasts clay	Strongly reactive	Smooth and gradual
P1C1	0.81-1.56	M	Sandy	10YR 8/1, 2.5YR 5/6	R	Carbonate, clay and quartz clasts	Strongly reactive	Smooth and abrupt
P1C2	1.56-2.78	M	Sandy (poorly selected)	10YR 8/1, 5YR 4/6, 5Y 8/6	R	Carbonate, clay and quartz clasts	Reactive	-
P2C1	0.00-2.65	M	Sandy (poorly selected)	5YR 7/4, 10YR 7/8, 10YR 8/1	A	-	Reactive	Smooth and abrupt
P2C2	2.65-3.04	M	Sandy (poorly selected)	10YR 8/1, 10R 3/6, 7.5YR 7/8, 5Y 2.5/1	R	-	Reactive	-

EST: structure; EB: blocky; M: massive; B: bioturbations; RHCl: reaction to hydrochloric acid; TRS: transition; A: abundant; R: rare.

Table 2. Morphological properties of the paleosols in the Piratininga Section (A2)

Profile and horizon	Depth	EST	Texture	Colors	B	Nodules	RHCl	TRS
	m							
P3C	0.00-4.50	M	Very fine sand to fine (BS)	5YR 7/4, 5YR 6/8, 2.5YR 4/8, 10YR 8/1	A	Sandy clasts with oxide films, nodule $CaCO_3$	RSR	-
P4-1C	2.30-2.90	M	Fine sandy bar to the average (MS)	5YR 7/4, 10YR 8/1	C	Clasts of quartz and clay	LRN	SC
P4-2C	2.90-3.50	M	Fine sandy bar to the average (MS)	5YR 8/3, 10YR 8/1, 2.5YR 5/8	C	Few clay clasts	NR	AS
P4-3C	3.50-4.50	M	Fine sandy bar to the average (MS)	5YR 8/3, 10YR 8/1, 5YR 7/6	C	Few clay clasts	NR	AS
P4-4C	4.50-4.90	M	Fine sandy bar to the average (MS)	5YR 8/3, 10YR 8/1, 5YR 7/6	C	Clay clasts	NR	AS
P4-5C	4.90-5.67	M	Fine sandy bar to the average (MS)	5YR 7/4, 2.5YR 4/8, 10YR 8/1	C	Clay clasts	NR	AS
P4-6C	5.67-6.64	M	Fine to coarse sand (SM)	5YR 8/3, 10YR 8/1, 5YR 7/6, 5YR 4/6	A	Carbonate, few clay clasts	R	SC
P4Bt1	6.64-7.42	P	Fine to medium sand (SMB)	5YR 7/4, 5YR 5/8, 10YR 8/1	CP	Clay clasts and carbonate nodules	R	SG
P5C1	0.00-3.20	M	Fine to medium sand (SMB)	5YR 7/4, 2.5YR 4/8, 10YR 8/1	A	Few clay clasts	R	SG
P5Bt1	3.20-3.56	PB	Fine to coarse sand (SM)	5YR 7/4, 2.5YR 5/8, 10YR 8/1	A	Few clay clasts	LR	SG
P5Bt2	3.56-4.18	PB	Fine to coarse sand (SM)	5YR 7/4, 2.5YR 6/8, 10YR 8/1	A	Clay nodules	RSR	SG
P5Btc	4.18-4.59	PM	Fine to coarse sand (SM)	5YR 7/4, 10YR 8/1	A	Few clay clasts	R	-
P6C1	0.00-1.19	M	Medium sand (SM)	5YR 7/4, 5YR 6/8, 10YR 8/1	A	Few clay clasts	LR	-
P7C1	0.00-0.28	M	Fine to medium sand (SMB)	5YR 6/6, 5YR 5/6, 2.5YR 4/8, 10R 6/4, 10YR 8/1	C	Few clay clasts	LR	AS
P7Btkm1	0.28-0.72	P	Fine to coarse sand (SM)	5YR 7/4, 2.5YR 5/6, 10YR 8/1	A	Abundant carbonate, clay clasts	R	SC
P7Btkmc	0.72-1.35	PM	Fine to coarse sand (SM)	5YR 7/4, 5YR 8/4, 2.5YR 6/8, 10YR 8/1	F	Abundant carbonate, clay clasts	RSR	-

EST: structure; M: massive; P: prismatic; PB: prismatic tending to block; PM: prismatic tending to massive; TRS: transition; BS: well selected; MS: poorly selected; SM: moderately selected; SMB: well to moderately selected; RHCl: reaction to hydrochloric acid; B: bioturbations; A: abundant; C: common; CP: common to few; F: few; RSR: reactive to strongly reactive; LRN: little reactive to nothing; NR: non-reactive; R: reactive; LR: little reactive; SC: smooth and clear; AS: smooth and abrupt; SG: smooth and gradual.

Interpretation of micromorphology

The way the fine material, the coarse material, and the voids are distributed provides clues regarding the origin and evolution of calcretes.

Interpretation of secondary processes of carbonate accumulation, such as substitution and recrystallization (Figures 5a, 6a and 7e), pattern diversity and degrees of physical and chemical weathering (Figures 5a, 5c, and 5e), root marks (Figures 6e and 7e), bioturbation (Figure 6c), *Microcodium* (Figure 7c), different nodules (Figures 6a and 7a), authigenesis of palygorskite (Figures 8a and 9), carbonate coating features (calcans) on quartz grains (Figure 7a and 7e) and clay coatings (Figure 8c and 8e), pisolite (Figure 10a), pending calcite (Figure 10c), and cytomorphic calcite (Figure 10e) showed the pedogenic origin of profiles.

Table 3. Morphological properties of the paleosols in the Garça Section (A3)

Profile and horizon	Depth	EST	Texture	Color	B	Nodule	RHCl	TRS
	m							
P8C1	0.72-2.72	Massive	Medium to coarse sand (poor selection)	5YR 7/4, 10YR 8/1, 2YR 7/6	Common	Sparse	Little reactive	AS
P8Bkm1	3.10-3.75	Laminar	Fine sand (moderate selection)	2.5YR 8/1, 2.5YR 7/4	Abundant	Abundant carbonate, few clay clasts	Reactive to strongly reactive	WC
P8Bkm2	3.75-4.36	Laminar	Fine sand (moderate selection)	10YR 5/4, 2.5YR 7/4, 10YR 8/1, 10YR 7/8	Abundant	Common carbonate, few clay clasts	Reactive	SC
P8Bk/Ck	4.36-4.63	Laminar tending to massive	Fine sand (moderate selection)	2.5YR 4/8, 5YR 7/4, 10YR 8/1	Rare	Few carbonate	Reactive	AS
P8Ckm1	4.63-5.31	Massive	-	-	Rare	-	-	AS
P9C1	0.00-1.18	Massive	Fine to coarse sand (poor selection)	5YR 7/3, 10YR 8/1, 2YR 7/6	Common	Rare carbonate, few clay clasts	Reactive	AS
P9Btkm	1.29-1.82	Prismatic	Fine sand (moderate selection)	5 YR 4/6, 5YR 7/4, 5YR 7/1, 7.5YR 8/6	Abundant	Few carbonate, scarce clay clasts	Reactive to strongly reactive	SC
P9Btkm/C	1.82-2.27	Prismatic tending to massive	Fine to medium sand (moderate selection)	5 YR 4/6, 5YR 7/4, 5YR 7/1, 7.5YR 8/6	Rare	-	Reactive	AS

EST: structure; B: bioturbations; RHCl: reaction to hydrochloric acid; TRS: transition; AS: smooth and abrupt; WC: wavy and clear; SC: smooth and clear.

The *microcodium* structures consist of cell aggregates composed of individual crystals of calcite (Kosir, 2004). Generally, *microcodium* is associated with the rhizogenic horizon (Figure 7c). Plant roots and microorganisms associated with the rhizosphere produce significant accumulations of calcium carbonate near the surface (Kosir, 2004). *Microcodium* occurs in petrocalcic horizons and calcretes, unlike rhizoliths, which normally occur in soil and sediments not completely cemented by calcium carbonate (Durand et al., 2010). This feature is associated with Cretaceous paleosol flood plains, lacustrine deposits, and paludal deposits (Durand et al., 2010). *Microcodium* structures (Figure 7c) are evidence of calcretes of pedogenic origin and indicate biologically controlled precipitation of calcium carbonate. Accumulations of *microcodium* probably reflect specific types of vascular plants of a pioneer community that had the ability to colonize carbonate substrates during the early phases of subaerial exposure (Kosir, 2004).

Groundmass features and pedofeatures have shown the predominance of *beta* type microfabrics in calcretes of the Marília Formation. *Beta* type microfabrics (biogenic/microbial related to the presence of roots, carbonates with alveolar fabric, fibrous calcite, *Microcodium*) and the presence of meniscus structures and pending cementation (pendant) are typical and striking features in pedogenic calcretes (Pimentel et al., 1996).

The calcite pendants (pending calcite) were another striking features in calcretes of the Marília Formation, manifesting their pedogenic origins. The pendants are laminated and composed of micritic and microsparitic calcite, with color ranging from light to dark brown (Figures 7e and 10c). Laminated pendants can reflect climate variations (Manafi and Poch, 2012). According to the authors, lighter colored blades, composed of relatively pure calcium carbonate, indicate dry periods, not suitable for biological activity. However, in more humid periods, climatic conditions become suitable for biological activity and the development of vegetation, increasing the production of organic matter, mixed with the calcium carbonate, resulting in darker stained

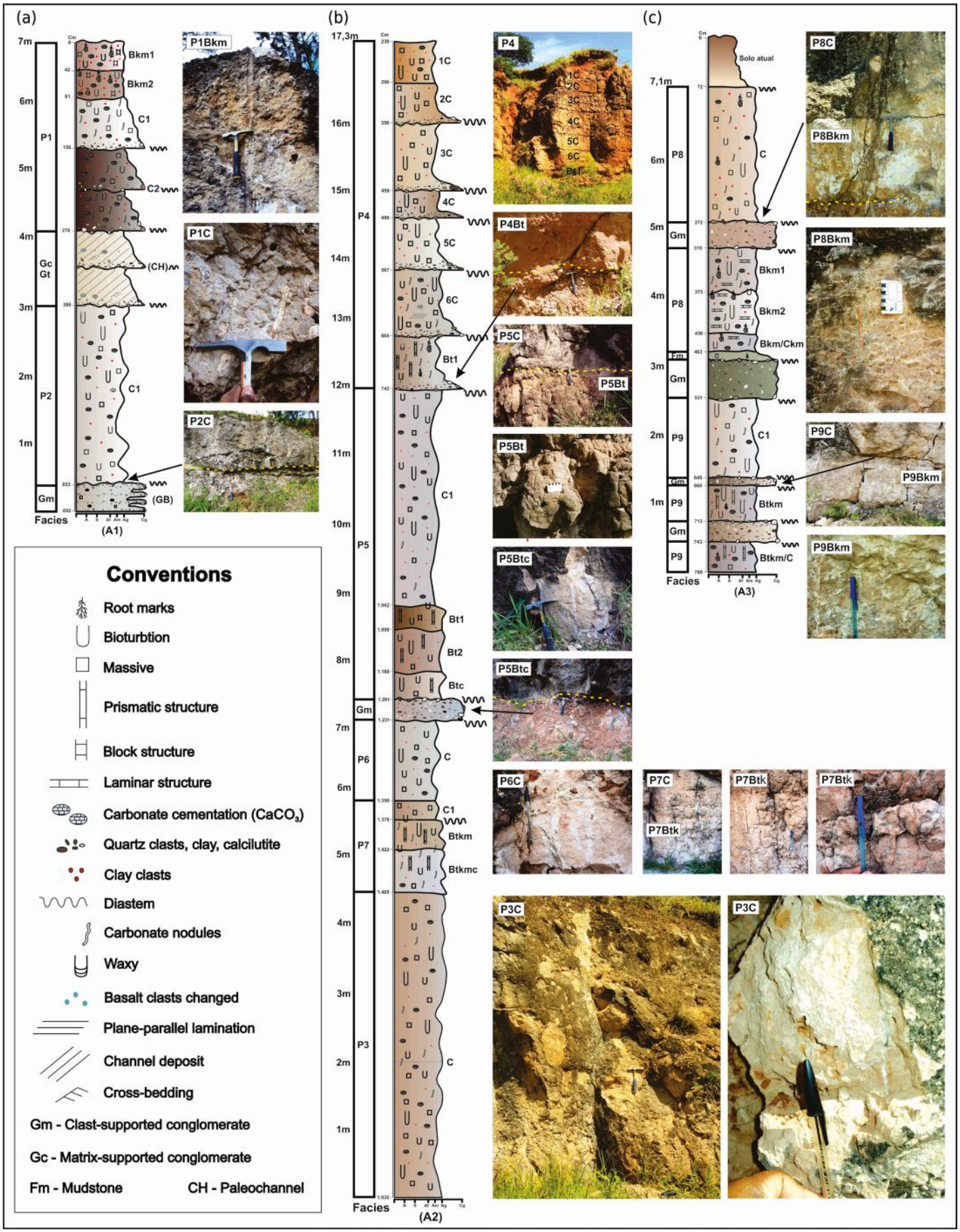

Figure 3. Facies association and macromorphology of paleosol profiles. (a) Column with the lithofacies (Gc, Gt, Gm) pedofacies (P1, P2), and paleosol profiles of the Botucatu section (A1) with its horizons; (b) Column with the lithofacies (Gm), pedofacies (P3, P4, P5, P6, P7), and paleosol profiles of the Piratininga section (A2) with its horizons; and (c) Column with the lithofacies (Gm, Fm), pedofacies (P8, P9) and paleosol profiles of the Garça section (A3) with its horizons.

Table 4. Synthesis of the fabric of the Bkm, Btkm, and Bt horizons of paleosols of the Marília Formation

Profile and horizon	Coarse material		Fine material		c/f-Related Distribution	GR	Pedofeature	Pedality
	Composition	Selection	Composition	FB				
P1Bkm	Qt (md), NF, Cal, Fel	MP	CC (d), MAOF	Ct	PA-Q-F	AA	HtgCe, PDCR, NTS	PBMDPA
P1Bkm2	Qt (md), PNF, Cal, Fel	MP	CC (d), MAOF	Ct	PA-Q	AA	HtgCe, PDCR, NTS	PBMFDAP
P4Bt1	Qt (md), PNF, FM	MB	CC, FMAOF	Gt, Pt, Me	PF-Q-E	ArA	RA, PDCR, NTS, PD	PPPFPA
P5Bt	Qt (md), PNF, Fel	MB	CC, FMAOF	Gt, Pt	PF-Q	AA	RA, PDCR, NTS, PD	PCMP
P5Bt2	Qt (md), PNF, Fel	M	CC, FMAOF	Gt, Pt	PF-Q	AA	RA, PDCR, NTS, PD	PCFP
P5Btc	Qt (md), PNF, Fel	M	CC, MAOF	Gt, Pt	PF-Q	ArA	RA, PDCR, NTS, PD	PCFP
P7Btkm1	Qt (md), PNF, Fel	M	CC (d), FMAOF	Gt	PF-Q	AA	RA, PDCR, NTS, HtgCe	PPPFPA
P7Btkmc	Qt (md), PNF, Fel, PB	M	CC (d), MAOF	Gt, Ct, Me, Sg	PF-Q	ArA	RA, PDCR, NTS, HtgCe	PCFP
P8Bkm1	Qt (md), PNF, Cal, Fel	M	CC (d), MAOF	Ct	PA	AA	HtgCe, PDCR, NTS	PLMFP
P8Bkm2	Qt (md), PNF, Cal, Fel	M	CC (d), MAOF	Ct	PA	AA	HtgCe, PDCR, NTS	PLMFP
P8Bkm/Ckm	Qt (md), PNF, Cal, Fel	M	CC (d), MAOF	Ct	PF-Q	AA	HtgCe, PDCR, NTS	PLFP
P9Btkm	Qt (md), NF, Cal, Fel, PB	M	CC (d), FMAOF	Pt, Gt, Sg	PF-Q-E	AA	RA, PDCR, NTS, HtgCe	PPMP
P9Btkm/C	Qt (md), PNF, Cal, Fel, PB	M	CC (d), MAOF	Ct, Pt, Gt, Sg	PF-E-Q	ArA	RA, PDCR, NTS, HtgCe	PPMP

FB: b-fabric; GR: particle size class; Qt (md): quartz very dominant; NF: common iron nodules; PNF: few iron nodules; Cal: calcite; Fel: feldspar fragments; FM: muscovite fragments; PB: very few biotite fragments; M: moderate; MB: moderate to good; MP: moderate to poor; CC (d): calcite cement dominant; CC: calcite cement; MAOF: clay minerals with iron oxides; FMAOF: common clay minerals with iron oxides; AA: sandy clay; ArA: loamy sand; PA: open porphyric; PF: closed porphyric; Q: chitonic; G: gefuric; E: enaulic; Ct: crystallitic; Pt: porostriated; Gt: granostriated; Sg: stipple-speckled; Me: monostriated; HtgCe: typical hypocoating grain by sparitic calcite; PDCR: dense infilling of root channel; PD: dense infilling; NTS: nodules typical and septaric; RA: clay coatings; PBMDPA: subangular blocky peds, moderately developed and partially accommodated; PBMFDAP: subangular blocky peds, moderately to weakly developed and partially accommodated; PPPFPA: pedal, prismatic, partially to strongly developed and partially accommodated; PCMP: pedal, complex (prismatic tending blocks), moderately developed and partially accommodated; PCFP: pedal, complex (prismatic tending blocks), poorly developed and partially accommodated; PLMFP: pedal, laminar, moderate to weakly developed and partially accommodated; PLFP: pedal, laminar, poorly developed and partially accommodated; PPMP: pedal, prismatic, moderately developed and partially accommodated.

blades (Manafi and Poch, 2012). In paleosols of the Marília Formation, the multilayer laminate of calcite pendant (Pt), indicated by yellow arrows (Figure 10c), point to improvement in moisture conditions. From this tone of brown, it may be inferred that climate conditions were more suitable for biological activity and development of vegetation, with production of organic matter, or the interpretation that the profile was under hydromorphic conditions.

In the paleosols of the Marília Formation, the amount of pending calcite increased in the Btkm horizons in relation to the Bkm of profiles 8 and 9.

Infillings and coatings were common features in calcretes (Figures 7e and 8). Coatings, hypocoatings, quasicoatings, and infillings are practically the result of pedological formation, the production of weathering (Stoops, 2008). There is partial alteration and replacement of quartz by microsparitic calcite coating (calcans), indicated by the yellow arrow (Figure 7e). Coating of quartz by carbonate is a typical feature of soil

profiles (Bedelean, 2004). According to Stoops (2008), the juxtaposition of (hypo) coatings allows chronology to be established, while analysis of the combination of fabric to determine the constituents enables micromorphology to identify the origin of the parent material or distinguish if the clay accumulations were formed by weathering or illuviation. The relative chronology of the paleosols of the Marília Formation (Figure 8e) suggested that there was initially carbonate coating, and then the clay was coated with iron oxide, a superimposing process (second stage). The chronological interpretation of

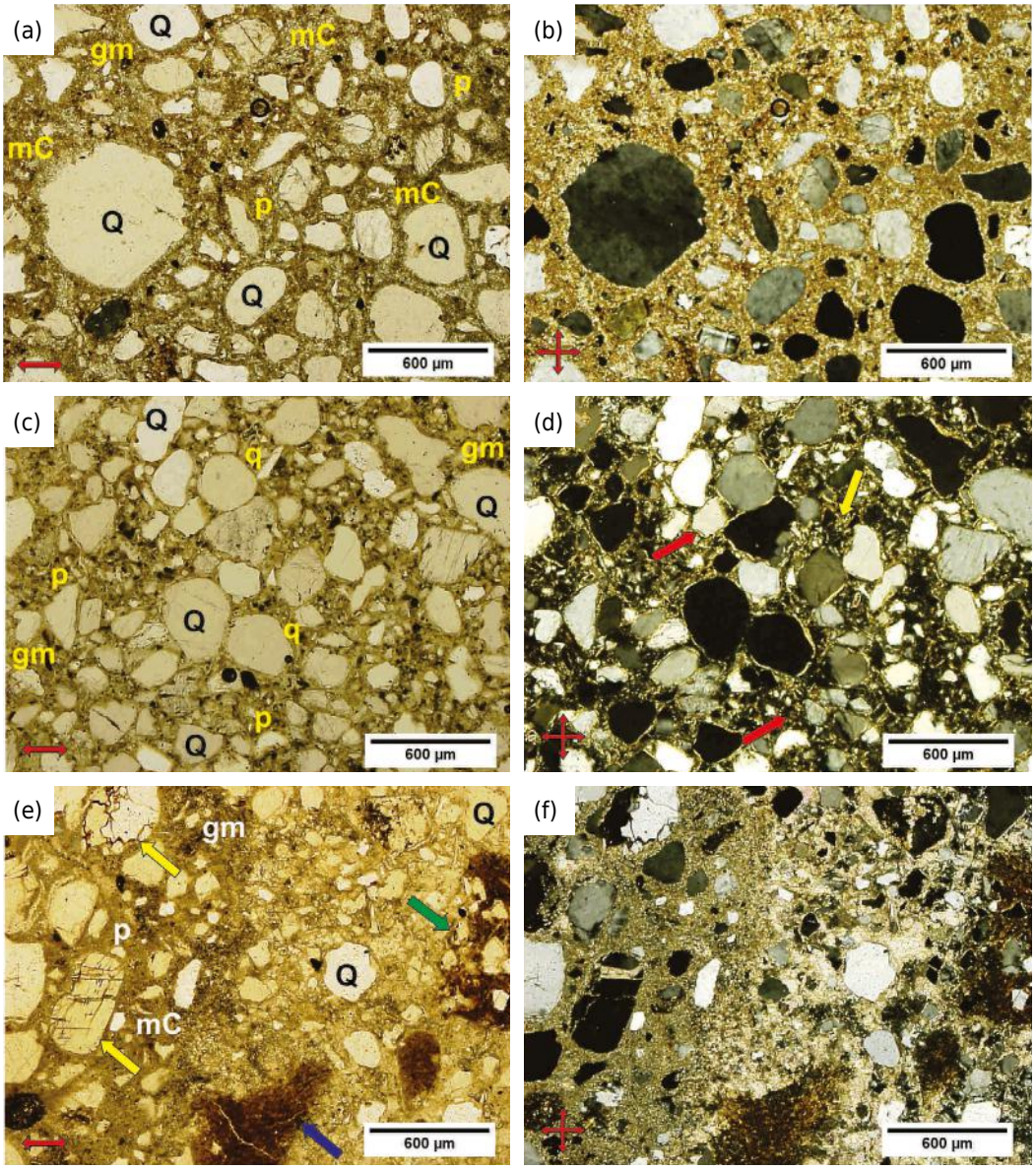

Figure 4. Aspects of groundmass (gm) of paleosols with Bkm, Bt, and Btkm horizons. (a) Groundmass Bkm1 horizon (P1). Coarse material consisting predominantly of quartz (Q) in blocky format, medium sand (200-500 µm), and moderate to poor selection. Fine material mainly composed of micritic calcite (mC). Porphyric related distribution (p); (b) Idem with crossed nicols (represented by the abbreviation NC, LP, or XPL); (c) Groundmass (gm) Bt1 horizon (P5) showing close porphyric- (p) and chitonic- (q) related distributions, highlighted in crossed nicols. The coarse material consists predominantly of quartz (Q) in blocky format. The fine material consists of cement $CaCO_3$ and clay minerals with iron oxides; (d) Idem with crossed nicols (NC, LP, or XPL). The red arrows identify granostriated and speckled b-fabric and yellow arrows identify clay coating; (e) Groundmass Btkm Horizon (P9) showing close porphyric-related distribution (p). In the groundmass, the coarse material consists predominantly of quartz (Q) in blocky format, while the fine material consists mainly of micritic calcite (mC) and clay minerals with iron oxides. Yellow arrows identify primary minerals in a physical-chemical weathering process. Iron nodule is indicated by the blue arrow; and clay coating is indicated through the green arrow; and (f) Idem with crossed nicols (XPL). Figures obtained by an optical microscope with a 2.5X objective and 100X eyepiece (250X magnification).

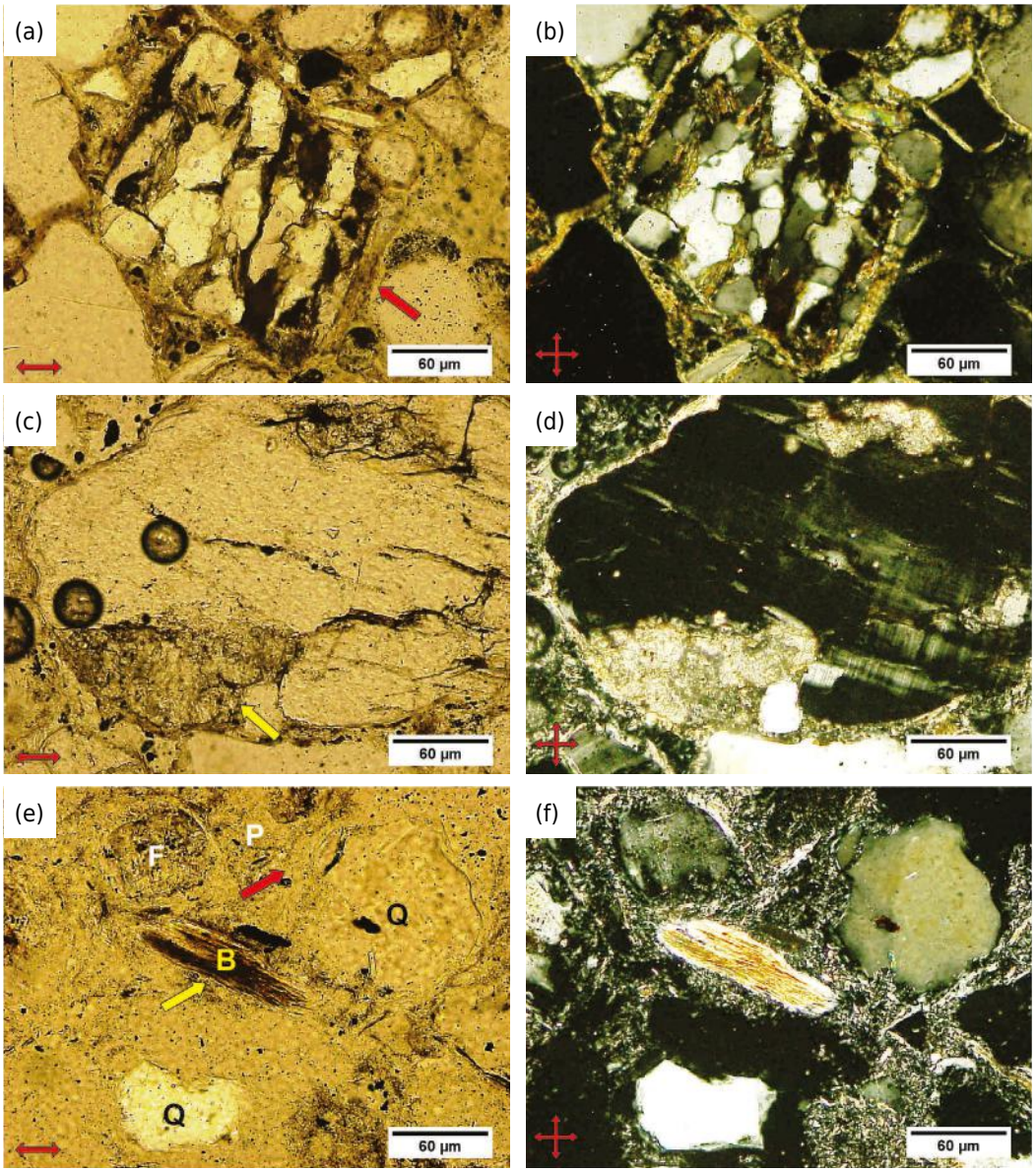

Figure 5. Alteration patterns and minerals replacement. (a) Concomitant process of weathering and replacement of polycrystalline quartz by calcite (red arrow) in the Bt1 horizon (P5). Silicate replacement process by calcite (epigenesis) is very common in horizons with high $CaCO_3$ content. The alkaline pH of these horizons causes a destabilization of quartz and its replacement by calcite, due to the opposite tendency in the solubility of silicon and carbonates as a function of the pH. In this replacement process called brecciation (indicated by the red arrow), the mineral grains are disintegrated into a series of separate fragments by the action of carbonates, but generally preserve the optical orientation of the original crystals. The quartz in the process of weathering presents a parallel linear and dotted alteration patterns with degree 3 (indicating that 75 to 97.5 % of the mineral was weathered); (b) Idem with XPL, a superimposition process of clayey material (iron oxides) on the carbonate features can be perceived with polarized light; (c) Partial alteration process with carbonate replacement in feldspar (Bk/Ck horizon – P8) (yellow arrow); feldspar shows irregular linear alteration pattern with degree 1 (indicating that 2.5 to 25 % of mineral was weathered); (d) Idem with XPL; (e) Parallel linear alteration pattern with degree 3 in biotite (B) of the Bkm1 horizon (P8) (yellow arrow); the red arrow indicates the dense discontinuous infilling feature (pedotubule), represented by the palygorskite mineral (P); Feldspar (F) is also present in the coarse material of the groundmass, as well as quartz (Q) in high proportions; and (f) Idem with XPL. Figures obtained by an optical microscope with a 10X objective and 100X eyepiece.

infilling also revealed that palygorskite (P) precipitated in the voids of paleosols, in the case of a secondary mineral (Figure 8a).

Carbonate coatings can be formed by evaporation or mechanical translocation or have their origins related to biological activity, consisting of microbial tubules or needle-like

calcite fibers (Stoops and Schaefer, 2010). These types of carbonate coatings were found in the paleosols of the Marília Formation (Figure 7). The red arrow indicated a product of carbonate reprecipitation around the quartz grain, which was a calcite coating (calcan) in paleosols of the Bkm horizon of the Marília Formation (Figure 7a).

Cytomorphic calcite was identified in profiles 8 and 9. This form of calcite develops under high biological activity and the presence of moisture (Manafi and Poch, 2012). The pedofeatures of carbonate depletion and accumulations of cytomorphic calcite are the result of biological activity in a wet climate, and are relics of a humid climate in the past (Manafi and Poch, 2012). Cytomorphic calcite composed of a sparitic carbonate decalcification zone found in the Btkm horizons of profile 9 (Figure 10e) can indicate transition from a drier climate to a more humid one, improvement in regional or local hydrological conditions, or that the profile was under hydromorphic conditions.

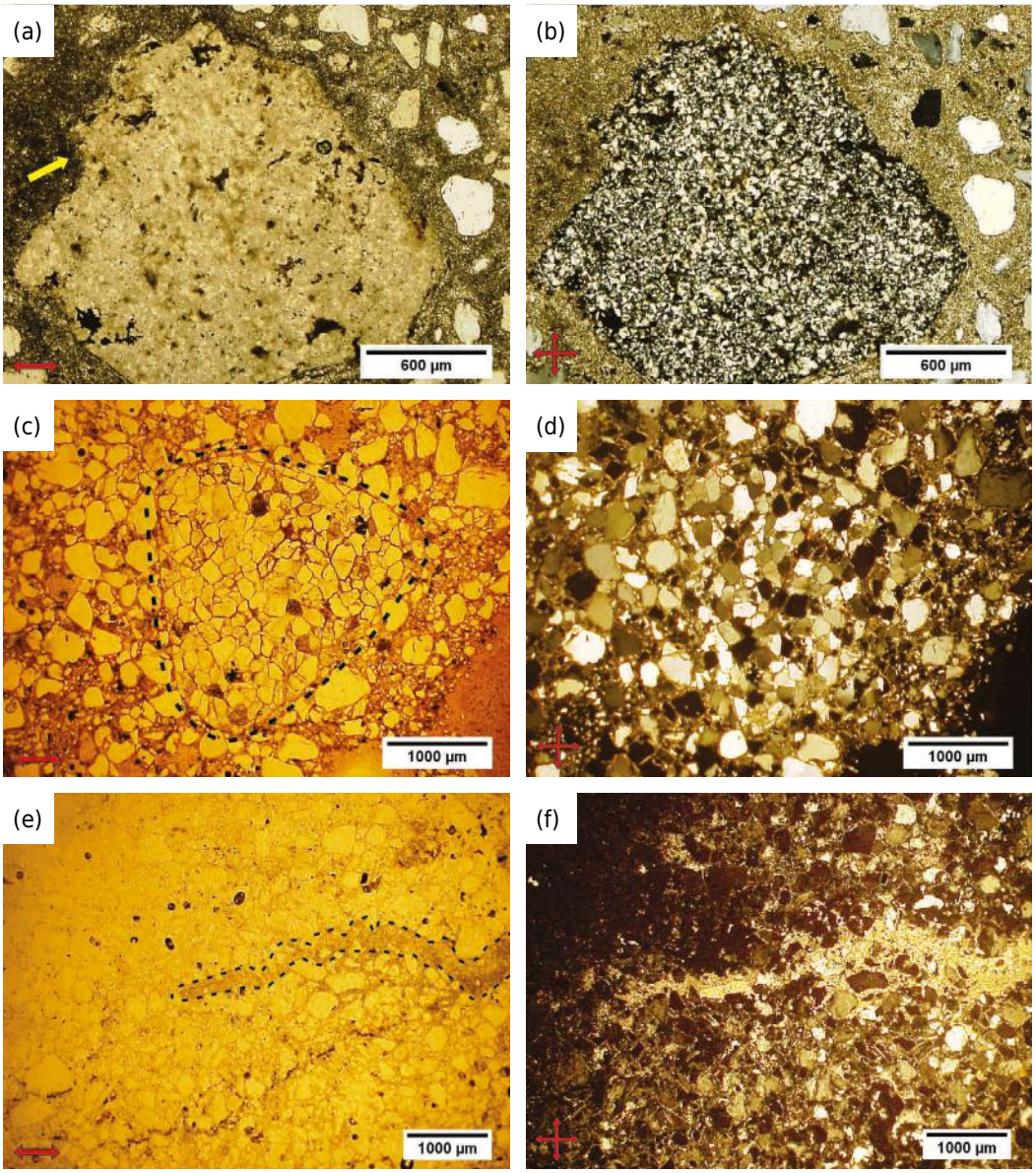

Figure 6. Recrystallization process and bioturbation features in paleosol horizons. (a) $CaCO_3$ recrystallization process in the C2 horizon (P1), resulting in a crystalline pedofeature (carbonate nodule with 1,768 µm) (yellow arrow); (b) Idem with XPL; (c) Bioturbation in the Bt1 horizon (P5), comprising a loose continuous infilling pedofeature with approximately 2,662 µm, filled with quartz grains (krotovine); (d) Idem with XPL; (e) Crystalline pedofeature, represented by the root mark (rhizolith $CaCO_3$) in the Bk/Ck horizon (P8); and (f) Idem with XPL. Images A and B were obtained by an optical microscope with a 2.5X objective and 100X eyepiece. Images (c), (d), (e), and (f) were obtained by a binocular loupe 2X (20X magnification).

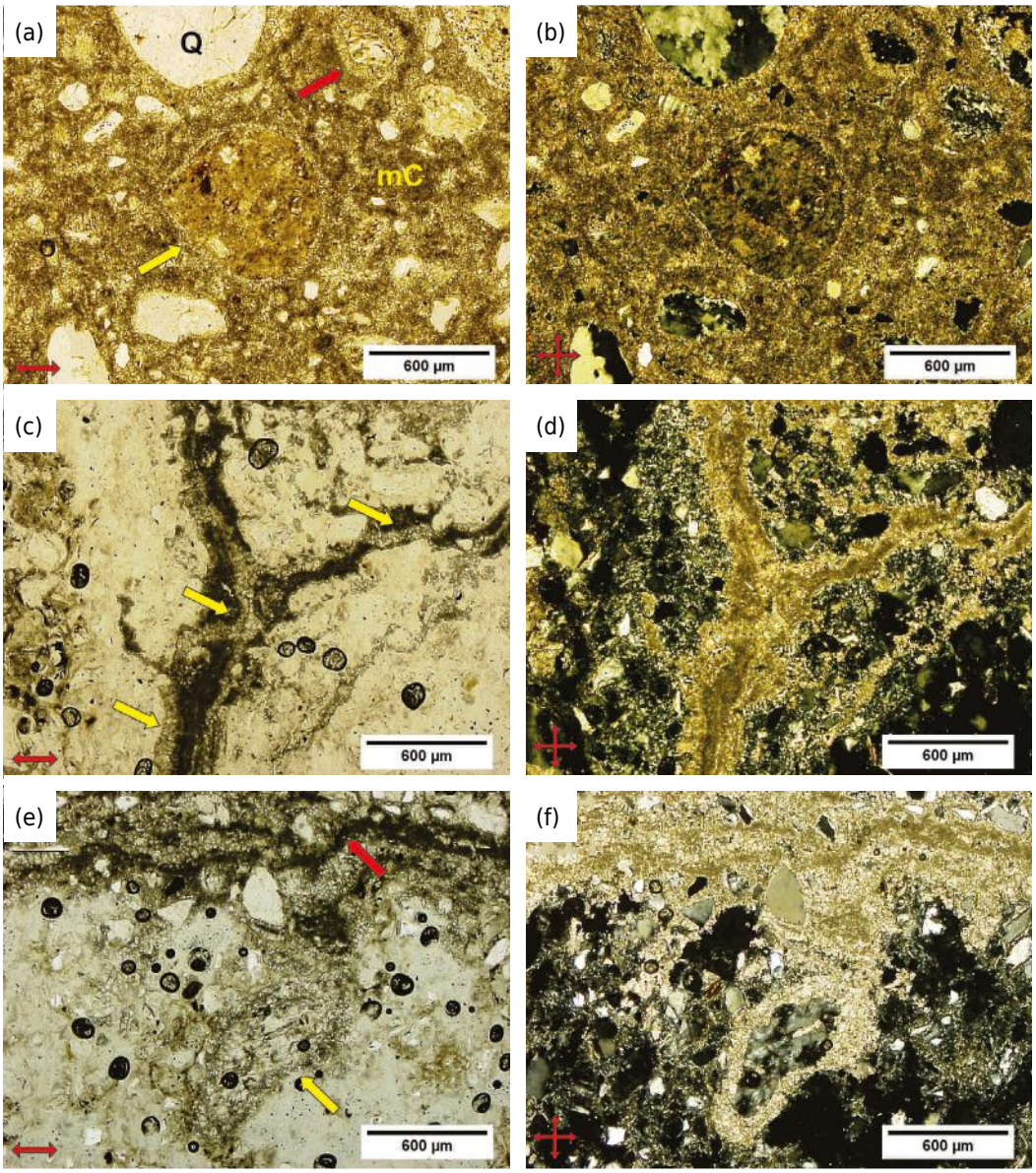

Figure 7. (a) Typical carbonate nodule strongly impregnated and stable with approximately 781 µm (yellow arrow) in the micritic cement (mC) of the Bkm1 horizon (P8); (b) Idem with XPL; (c) *Microcodium* in the Bkm1 horizon (P8) (arrows); (d) Idem with XPL; (e) Replacement process and bioturbation feature in laminar Bkm1 horizon (P8); and (f) Idem with XPL. The red arrow indicates a calcified root mark, common in rhizogenic calcrete (consisting of calcite pendant, indicative moisture and high biological activity). Figures obtained by an optical microscope with a 2.5X objective and 100X eyepiece.

However, calcification-decalcification pedofeatures associated with impregnating the root tissue is often observed in semi-arid calcareous soils (Durand et al., 2010). This feature, according to the authors, corresponds to infillings of channels by cytomorphic sparitic calcite, surrounded by a zone of non-calcareous material.

Another pedofeature found in Bt horizons was pisolite (Figure 10a). Pisolites are common in highly developed petrocalcic horizons or calcretes (Phases V and VI of Machette (1985) when the calcic horizon is hardened and subject to pedogenesis and alteration by physical and chemical weathering (Durand et al., 2010). Concentric bands of clay in pisolites may result from clay neoformation with Si and Al, and these concentric layers may indicate control by microorganisms associated with roots (Durand et al., 2010).

In paleosols of the Marília Formation, the carbonate character was confirmed by the predominance of porphyric-related distribution and crystallitic b-fabric in the

groundmass (Figure 4a). Crystallitic b-fabric can develop when fine calcite crystals gradually precipitate in the micromass of clay and when the pore space between the grains is progressively filled by pedogenic carbonate crystals with a particle size between clay and silt (Stoops and Schaefer, 2010). Identification and interpretation of porphyric-chitonic related distribution, speckled-porostriated b-fabric, and clay coatings have shown the features of argillic horizons in the paleosols with a Bt horizon defined in the field (Figures 4c, 4e, 8c, and 8e).

Gefuric-related distributions identified in paleosols indicated aggradation (training) for illuviation and enaulics, an increased pedogenesis process, and stability of the environment. Chitonic-related distributions are results of a poor illuviation process in

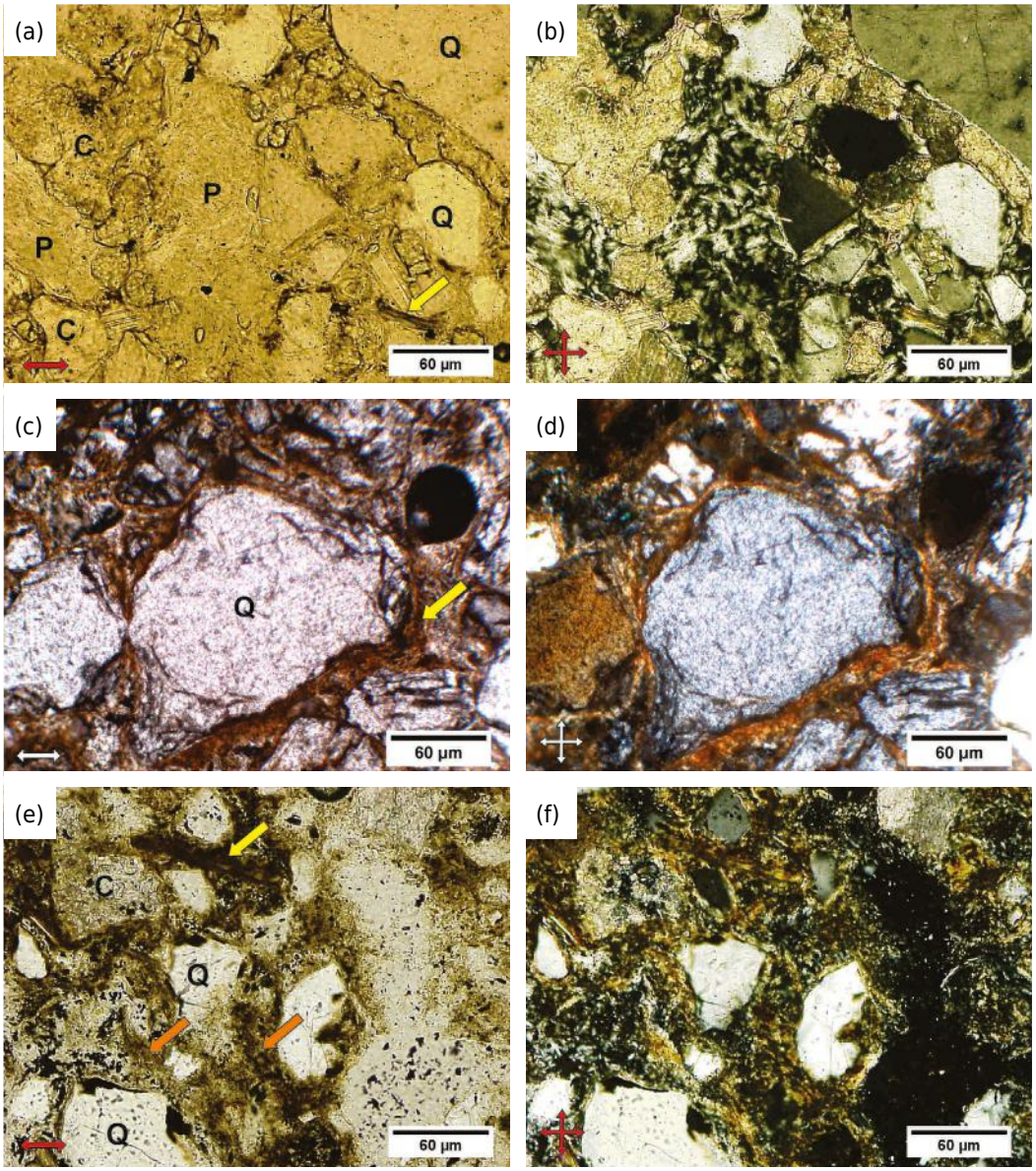

Figure 8. (a) Chronology and hierarchical aspects of the Bkm horizon (P1). The hierarchy shows quartz grains (Q), microsparitic calcite (C), and palygorskite (P) at the first level, which is in the groundmass (second level). The yellow arrow indicates an altered biotite; (b) Idem with XPL; (c) Pedofeature coating in the Bt2 horizon (P5). The yellow arrow indicates a clay coating with iron oxides around the quartz grains (Q), typical autochthonous pedofeature. You can see the orientation of the illuvial process of the clay product; (d) Idem with XPL; (e) Aspect of the groundmass (hierarchy and chronology) and pedofeatures of the Btkm horizon (P9); and (f) Idem with XPL. Orange arrows show clay coatings with iron oxides (autochthonous pedofeatures), and yellow arrows show a weathered biotite. Around the biotite can be seen pedoplasmation processes with granostriated b-fabric. Figures obtained by an optical microscope with a 10X objective and 100X eyepiece.

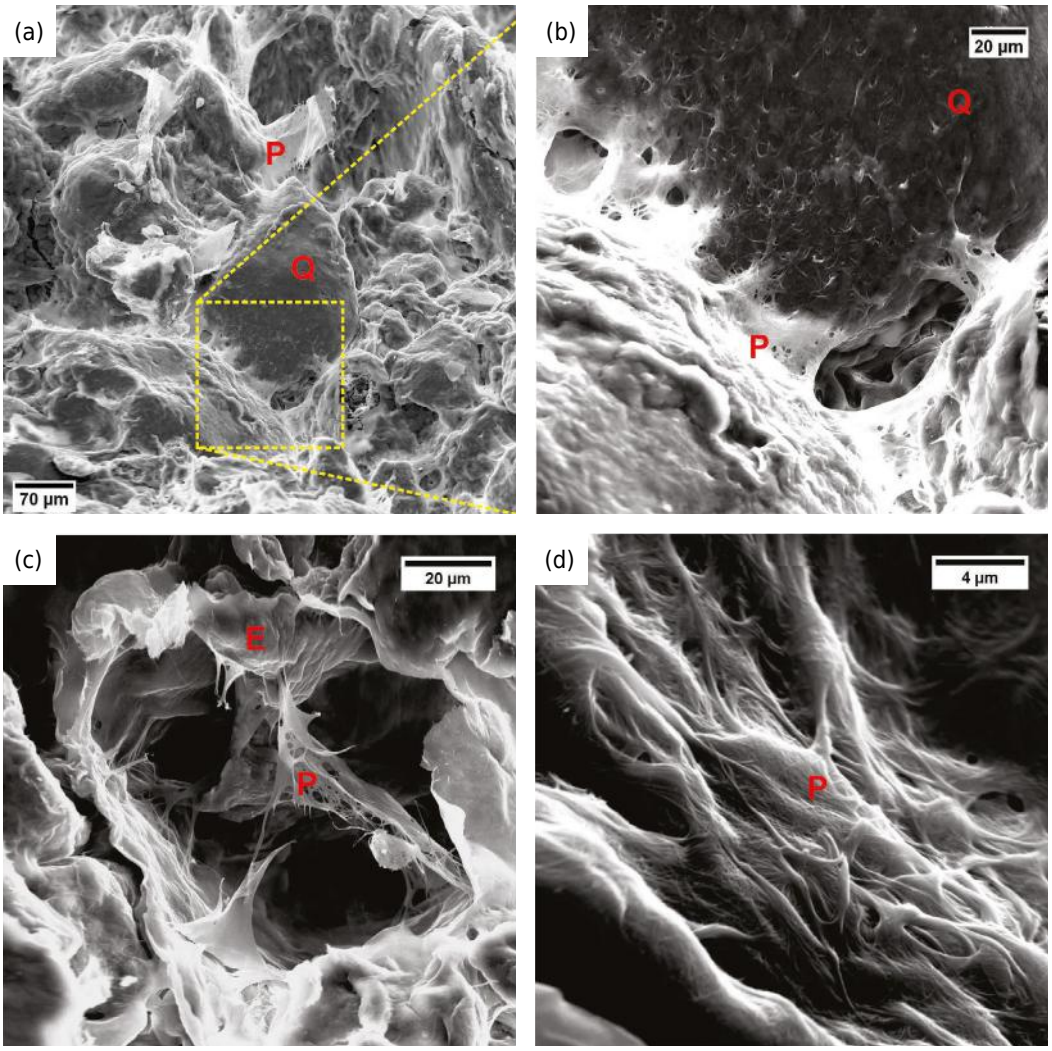

Figure 9. Scanning electron microscopy of the C1 horizon (P3). (a) Authigenesis of palygorskite (P), coating grains of quartz (Q) and calcite; (b) Detail of palygorskite (P) in the form of aggregates of entangled fibers coating the quartz grain (Q); (c) Formation of palygorskite (P) through the alteration of the smectite (E); palygorskite in the form of aggregate filling the voids of intertwined fibers can be observed, a typical feature of paleosols (Singer, 2002); and (d) Detail of fibrous aggregate with woven wire and with some guidance from palygorskite.

paleosols. Porphyric- related distribution indicated initial change and strong cementation of grains per illuviation.

Crystallitic b-fabrics in Bk horizons (Figure 4a) were formed by crystallization of relatively soluble parts of the fine material, while the speckled b-fabrics (Figures 4c, 4e, and 8e) indicated *in situ* weathering of primary minerals. Porostriated and granostriated b-fabrics (Figures 4c, 4e, and 8e) indicated pressure in the voids and grains.

The evolution of pedogenic processes, in light of micromorphological analysis, evidenced three moments or stages to the genesis of paleosols. In the drier first stage, there is intense cementation of horizons with micritic and microsparitic calcite (generating porphyric c/f-related distribution) and palygorskite precipitation in the voids or filling bioturbations (Figures 4a, 6a, 6e, 7e, 8a, and 9). The second phase is characterized by the destruction of porphyric-related distributions for establishing chitonic and enaulic-related distributions (Figures 4e and 8e). Relative chronology revealed a superimposition of the features of iron oxides on carbonate cementation (Figure 8e). In the third local or regional wetter phase, carbonate cementation no longer exists, giving way to advancement of chitonic- and gefuric-related distributions, resulting in paleosols with Bt (Figures 4c, 8c, and 10a).

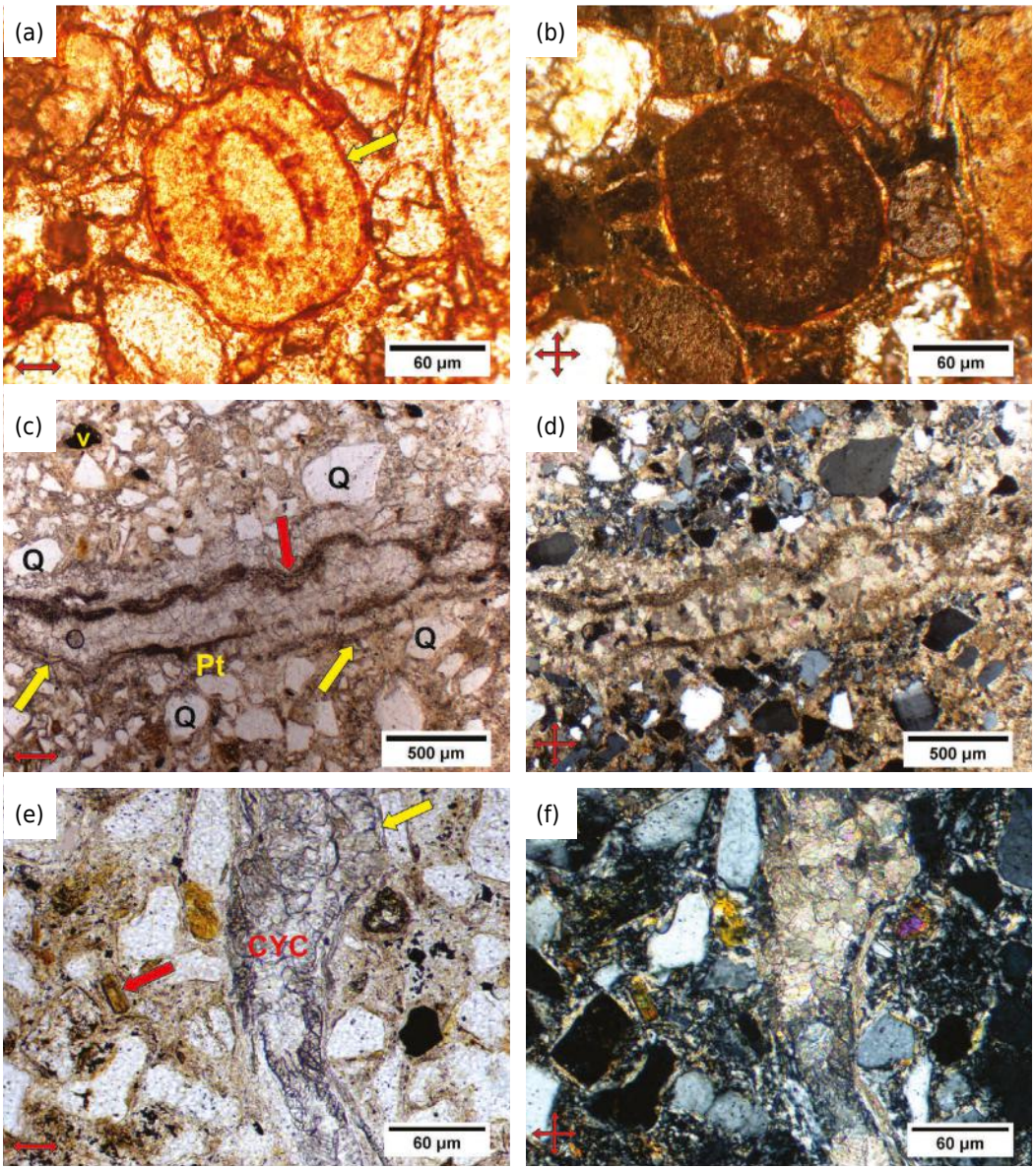

Figure 10. (a) Pisolite showing concentric rings of iron-containing materials (Bt1 horizon - P5), with natural light (represented by the abbreviation LN or PPL). The yellow arrow also shows clay with iron oxides coating the pisolite. You can see the presence of chitonic/enaulic-related distribution (partially evidenced by the yellow arrow); (b) Idem with XPL; (c) Calcite pendant (pending calcite) in the Btkm horizon (P9), below the quartz grains (Q), indicated by the red arrow. The layers are pending calcite between the quartz grains (Q) and in the upper left portion, a porosity channel (v) can be seen; (d) Idem with XPL; (e) Cytomorphic Calcite (CYC) in the Btkm horizon (P9), indicated by the yellow arrow. The red arrow identifies a biotite, with little change; and (f) The decalcification zone, highlighted with crossed nicols, around the root channel filled by cytomorphic calcite (CYC) can be observed. Figures (a), (b), (e) and (f) obtained by an optical microscope with a 10X objective and 100X eyepiece (1000 times magnification). Figures (c) and (d) were obtained with an objective of 2.5X.

In the Maastrichtian of the Bauru Basin, the interpretation of micromorphology showed that paleosols with a Bkm horizon are older and more arid environments. After that, the paleosols are coated by clay minerals with iron oxides, culminating in the destruction of porphyric-related distributions (carbonate cementation) and the establishment of chitonic-related distributions in wetter local or regional climatic conditions, generating paleosols with a Bt horizon. However, these climate conditions, although more hot and humid, were not enough to generate enaulic-related distributions, typical of current Oxisols.

The genesis of paleosols with Bt horizons predates the establishment of higher humidity and temperature conditions that were established in the Tertiary Period.

CONCLUSIONS

Analysis and interpretation of the macro- and micromorphology suggested different conditions of weathering and leaching in the evolution of the Marília Formation, resulting in paleosols with Bkm, Btkm, and Bt horizons.

The paleosols with Bkm were formed first, under drier conditions. The second stage was characterized by destruction of porphyric-related distributions and formation of chitonic- and gefuric-related distributions.

The third stage was probably wetter and there was advancement of chitonic- and gefuric-related distributions, and formation of paleosols with Bt.

These results suggest climatic cyclicality or changes in the hydrology of the basin during the Maastrichtian.

ACKNOWLEDGMENTS

The authors are thankful for the support of the Federal Institute of Education, Science and Technology of the South of Minas Gerais, Inconfidentes *Campus*, and the Graduate Studies Program in Geosciences of the Geosciences Institute of the University of Campinas; and for the financial support of the São Paulo Research Foundation (FAPESP Project 2015/17632-5).

REFERENCES

Amaral G, Bushee J, Cordani UG, Kawashiita K, Reynolds JH. Potassium-argon ages of alkaline rocks from Southern Brazil. Geochim Cosmochim Acta. 1967;31:117-42.

Andreis RR. Identificación e importancia geológica de los paleosuelos. Porto Alegre: Universidade Federal do Rio Grande do Sul; 1981.

Batezelli A, Saad AR, Basilici G. Arquitetura deposicional e evolução da seqüência aluvial neocretácea da porção setentrional da bacia Bauru, no sudeste brasileiro. Rev Bras Geocienc. 2007;37:163-81.

Batezelli A. Análise da sedimentação cretácea no triângulo mineiro e sua correlação com áreas adjacentes [tese]. Rio Claro: Universidade Estadual Paulista; 2003.

Batezelli A. Arcabouço tectono-estratigráfico e evolução das bacias Caiuá e Bauru no sudeste brasileiro. Rev Bras Geocienc. 2010;40:265-85.

Batezelli A. Continental systems tracts of the Brazilian Cretaceous Bauru Basin and their relationship with the tectonic and climatic evolution of South America. Basin Res. 2015;27:1-25. doi:10.1111/bre.12128

Bedelean H. Study on the diagenetic calcareous accumulations in a soil profile from Florestin (Cluj country, Romania). Studia UBB, Geologia. 2004;69:75-85. doi:10.5038/1937-8602.49.1.7

Birkeland PW. Soil and geomorphology. 3rd ed. New York: Oxford University Press; 1999.

Brown TM, Kraus MJ. Pedofacies analysis: a new approach to reconstructing ancient fluvial sequences. In: Reinhardt J, Sigleo WR, editors. Paleosols and weathering through geologic time: principles and applications. Boulder: Geological Society of America; 1988. p.143-52.

Bullock P, Fedoroff N, Jongerius A, Stoops G, Tursina T. Handbook for soil thin section description. London: Waine Research Publications; 1985.

Castro SS, Cooper M, Santos MC, Vidal-Torrado P. Micromorfologia do solo: bases e aplicações. Tópic Cienc Solo. 2003;3:107-63.

Catt JA. Paleopedology manual. London: Pergamon; 1990.

Delvigne JE. Atlas of micromorphology of mineral alteration and weathering. Ontario: Mineralogical Association of Canada; 1998.

Dias-Brito D, Musacchio EA, Castro JC, Maranhão MSAS, Suarez JM, Rodrigues R. Grupo Bauru: uma unidade continental Cretácea no Brasil - concepções baseadas em dados micropaleontológicos, isotópicos e estratigráficos. Rev Paleontol Eobiol. 2001;20:245-304.

Durand N, Monger HC, Canti MG. Calcium carbonate features. In: Stoops G, Marcelino V, Mees F, editors. Interpretation of micromorphological features of soils and regoliths. Amsterdam: Elsevier; 2010. p.149-94.

Fernandes LA, Coimbra AM. A Bacia Bauru (Cretáceo Superior, Brasil). Anais Acad Bras Cienc. 1996;68:195-205.

Fernandes LA, Coimbra AM. Revisão estratigráfica da parte oriental da bacia Bauru (Neocretáceo). Rev Bras Geocienc. 2000;30:717-28.

Fernandes LA. Mapa litoestratigráfico da parte oriental da bacia do Bauru (PR, SP, MG), escala 1:1.000.000. Bol Paranaense Geocienc. 2004;55:53-66.

Fitzpatrick EA. The micromorphology of soils. Aberdeen: University of Aberdeen; 1984.

Fragoso CE, Weinschutz LC, Vega CS, Guimarães GB, Manzig PC, Kellner AW. Short note on the pterosaurs from the Caiuá Group (Upper Cretaceous, Bauru Basin), Paraná State, Brazil. In: International Symposium on Pterosaurs; 2013; Rio de Janeiro. Rio de Janeiro: UFRJ; 2013. p.71-2.

Fulfaro VJ, Etchebehere MLDC, Perinotto JAJ, Saadi AR. Santo Anastácio: um geossolo cretácico na bacia Caiuá. In: Anais do 5º Simpósio sobre o cretáceo do Brasil; 1999; Serra Negra. Rio Claro: UNESP; 1999. p.125-30

Fulfaro VJ, Perinotto JAJ. A bacia Bauru: estado da arte. In: Boletim do 4° Simpósio sobre o Cretáceo do Brasil; 1996; Rio Claro. São Paulo: UNESP; 1996. p.297-303.

Gile LH, Peterson FF, Grossman RB. Morphological and genetic sequences of carbonate accumulation in desert soils. Soil Sci. 1966;101:347-54.

Gobbo-Rodrigues RS. Carófitas e Ostracódes do Grupo Bauru [tese]. Rio Claro: Universidade Estadual Paulista; 2001.

Guimarães GB, Liccardo A, Godoy LC, Weinshutz, LC, Manzig PC, Vega CS, Pilatti F. Ocorrência de Pterossauros no Cretáceo da Bacia do Paraná/Bauru: implicações para a geoconservação, paleontologia e estratigrafia. In: 46th Geology Brazilian Congress; 2012; Santos. Santos: SBG; 2012.

Hartley AJ, Weissman GS, Nichols G, Warwick GL. Large distributive fluvial systems: characteristics, distribution and controls on development. J Sedim Res. 2010;80:167-83. doi:10.2110/jsr.2010.016

Hasui Y, Cordani UG. Idades potássio-argônio de rochas eruptivas mesozóicas do este mineiro e sul de Goiás. In: 2nd Brazilian Geology Congress Bulletim; 1968; Belo Horizonte. Belo Horizonte: SBG; 1968. p.139-43.

Kosir A. Microcodium revisited: root calcification products of terrestrial plants on carbonate-rich substrates. J Sedim Res. 2004;74:845-57.doi:10.1306/040404740845

Kraus MJ. Alluvial response to differential subsidence: sedimentological analysis aided by remote sensing, Wilwood Formation (Eocene), Bighorn basin, Wyoming, USA. Sedimentology. 1992;39:455-70.

Kraus MJ. Lower Eocene alluvial paleosols: pedogenic development, stratigraphic relationships, and paleosol/landscape associations. Palaeogeog Palaeoclimatol Palaeoecol. 1997:129:387-406. doi:10.1016/S0031-0182(96)00056-9.

Machado Junior DL. Idades Rb/Sr do complexo alcalino-carbonatítico de Catalão II (GO). In: 29th Brazilian Geology Congress Bulletim; 1992; São Paulo. São Paulo: SBG; 1992. p.91-3.

Machette MN. Calcic soils of the southwestern United States. Geol Soc Am Bull. 1985; Special Paper:1-21.

Manafi S, Poch RM. Micromorphic pedofeatures related to pedogenic calcium carbonate in some arid and semiarid soils in the west of Urmia Lake, Iran. In: Proceedings of the 14th International Working Meeting on Soil Micromorphology; 2012; Lleida. Lleida: SECS; 2012.

Marriott SB, Wright VP. Palaeosols as indicators of geomorphic stability in two Old Red Sandstone alluvial suites, South Wales. J Geol Soc. 1993;150:1109-20. doi:10.1144/gsjgs.150.6.1109

Martinelli AG, Rief D, Lopes RP. Discussion about the occurrence of the genus Aeolosaurus Powell 1987 (Dinosauria, Titanosauria) in the Upper Cretaceous of Brazil. GAEA J Geosci. 2011;7:34-40. doi:10.4013/gaea.2011.71.03

Mccarthy P, Plint G. Spatial variability of palaeosols across Cretaceous interfluves in the Dunvegan Formation, NE British Columbia, Canada: palaeohydrological, palaeogeomorphological and stratigraphic implications. Sedimentology. 2003;50:1187-220. doi:10.1111/j.1365-3091.2003.00600.x

Nascimento NL, Ladeira FSB, Batezelli A. Pedodiagenetic Characterization of Cretaceous Paleosols in Southwest Minas Gerais, Brazil. Rev Bras Cienc Solo. 2017;41:e0160065. doi: 10.1590/18069657rbcs20160287

Paula and Silva F, Chang HK, Caetano-Chang MR.Estratigrafia de subsuperfície do Grupo Bauru (k) no estado de São Paulo. Rev Bras Geocienc. 2005;35:77-88.

Pimentel NL, Wright VP, Azevedo TM. Distinguishing early groundwater alteration effects from pedogenesis in ancient alluvial basins: examples from the Palaeogene of southern Portugal. Sedim Geol. 1996;105:1-10. doi:10.1016/0037-0738(96)00034-6

Porta J, López-Acevedo M, Roquero C.Edafología para la agricultura y el medio ambiente. 3rd ed. Madri: Mundi-Prensa Libros; 1999.

Retallack GJ. Field recognition of paleosols. GSA Sp Paper. 1988;216:1-20.

Retallack GJ. Soils of the past: an introduction to paleopedology. 2nd ed. London: Unwin Hyman; 2001.

Riccomini C. Arcabouço estrutural e aspectos do tectonismo gerador e deformador da bacia Bauru no estado de São Paulo. Rev Bras Geocienc. 1997;27:153-62.

Riccomini C. Tectonismo gerador e deformador dos depósitos sedimentares pós-gondwânicos da porção centro-oriental do estado de São Paulo e áreas vizinhas [livre-docência]. São Paulo: Universidade de São Paulo; 1995.

Santos RD, Lemos RC, Santos HG, Ker JC, Anjos LHC. Manual de descrição e coleta de solo no campo. 5a ed. Viçosa, MG: SBCS; 2005.

Santucci RM, Bertini RJ. Distribuição paleogeográfica e biocronológica dos Titanossauros (Saurishia, Sauropoda) do Grupo Bauru, Cretáceo Superior do sudeste brasileiro. Braz J Geol. 2001;31:307-15.

Sheldon ND, Tabor NJ. Quantitative paleoenvironmental and paleoclimatic reconstruction using paleosols. Earth Sci Rev. 2009;95:1-52. doi:10.1016/j.earscirev.2009.03.004

Singer A. Palygorskite and sepiolite. In: Dixon JB, Schulze DG, editors. Soil mineralogy with environmental applications. 2nd ed. Wisconsin: SSSA Book Series; 2002. p.556-84.

Sonoki IK, Garda GM. Idades K-Ar de rochas alcalinas do Brasil Meridional e Paraguai Oriental: compilações e adaptação às novas constantes de decaimento. Geosci Inst Bull. 1988;19:63-85.

Stanistreet I, Mccarthy TS. The Okavango fan and the classification of sub aerial fan systems. Sedim Geol. 1993;85:115-33.doi:10.1016/0037-0738(93)90078-J

Stoops G, Marcelino V, Mees F, editors. Interpretation of micromorphological features of soils and regoliths. Amsterdam: Elsevier; 2010.

Stoops G, Schaefer CEGR. Pedoplasmation: formation of soil material. In: Stoops G, Marcelino V, Mees F, editors. Interpretation of micromorphological features of soils and regoliths. Amsterdam: Elsevier; 2010. p.69-79.

Stoops G. Guidelines for analysis and description of soils and regolith thin sections. Madison: Soil Science Society of America; 2003.

Stoops G. Micromorphology. In: Chesworth W, editor. Encyclopedia of soil science. New York: Springer; 2008. p.457-66.

Wright VP. Paleopedology: Stratigraphic relationship and empirical models. In: Martini IP, Chesworth W, editors. Weathering, soils and paleosols. Amsterdan: Elsevier; 1992. p.475-99.

Wright VP. Paleosols: their recognition and interpretation. Princeton: Princeton University Press; 1986.